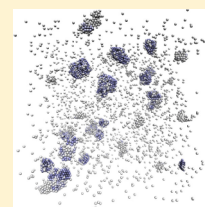


Monodisperse Clusters in Charged Attractive Colloids: Linear Renormalization of Repulsion

Štěpán Růžička^{*,†,‡} and Michael P. Allen^{‡,§}[†]Laboratoire de Physique des Solides, Université Paris-Sud and CNRS, UMR 8502, 91405 Orsay, France[‡]Department of Physics, University of Warwick, Coventry CV4 7AL, United Kingdom[§]H. H. Wills Physics Laboratory, University of Bristol, Royal Fort, Tyndall Avenue, Bristol BS8 1TL, United Kingdom

S Supporting Information

ABSTRACT: Experiments done on polydisperse particles of cadmium selenide have recently shown that the particles form spherical isolated clusters with low polydispersity of cluster size. The computer simulation model of Xia et al. (*Nat. Nanotechnol.* **2011**, *6*, 580) explaining this behavior used a short-range van der Waals attraction combined with a variable long-range screened electrostatic repulsion, depending linearly on the volume of the clusters. In this work, we term this dependence “linear renormalization” of the repulsive term, and we use advanced Monte Carlo simulations to investigate the kinetically slowed down phase separation in a similar but simpler model. We show that amorphous drops do not dissolve and crystallinity evolves very slowly under linear renormalization, and we confirm that low polydispersity of cluster size can also be achieved using this model. The results indicate that the linear renormalization generally leads to monodisperse clusters.



1. INTRODUCTION

Designing nanoparticles for self-assembly¹ is a step toward controlled and ecological fabrication of colloidal crystals with remarkable material properties.^{2,3} Many colloidal systems, at low volume fraction, phase separate into colloidal clusters.^{4,5} Short-range attractive colloidal systems at low volume fraction are known to form metastable clusters after quenches to low temperatures.^{6,7} Clustering is initiated by spinodal decomposition and followed by competition of thermodynamics and kinetics.^{8,9} If the cluster motion is slow or inhibited, the clusters remain isolated for a very long time,^{7,8} and local order evolves either via recrystallization⁴ or dissolution¹⁰ of amorphous clusters, where single-particle exchange (Ostwald ripening) is the dominant mechanism for dissolution and growth. If the clusters are allowed to move, the kinetics may lead to the formation of gels,^{8,11} which may recrystallize afterward. This aggregation can be slowed down¹⁰ or completely avoided,¹² if the colloids are charged, and cluster phases emerge.^{5,13} Nevertheless, addition of long-range repulsion to the short-range attraction may lead to several complications. First, the energy landscape of the system has more basins,^{14,15} and hence more possible kinetic traps. Zhang et al.¹⁶ have recently argued that long-living cluster states observed both in simulations and in experiments are not equilibrium states. Mani et al.¹⁷ have then shown that equilibrium cluster phases may be expected only if the attraction strength is such that bonds can break and re-form.¹⁸ Second, the kinetic slowing down observed in models of short-range attractive and long-range repulsive (SALR) particles may just be caused by kinetically realistic dynamical or Monte Carlo simulations which do not have access to the long times needed to escape the kinetic traps. Although basin hopping techniques were used to find ground states of individual clusters,¹⁹ it is known that if many such

clusters are mixed in a fixed volume, the long-range interactions change their internal structure.^{20,21} To our knowledge, the only simulation study investigating the thermodynamic stability of a SALR system composed of several clusters was the work of Charbonneau and Reichman,¹² who used nonkinetic Monte Carlo moves and a small SALR two-dimensional system to show that gelation in those systems is also a consequence of arrested phase separation.¹¹ The polydispersity of their small stable clusters was not investigated systematically; nevertheless, the snapshot in their work indicates that the clusters are not monodisperse. Sweatman et al.²² have recently specified conditions under which large spherical monodisperse clusters are thermodynamically stable and where the kinetic arrest in SALR systems can be avoided by longer-range attraction.

In this work, we study an SALR system, where the repulsion amplitude is linearly proportional to the volume of the clusters accommodating the particle pair. This renormalization is based on the one used by Xia et al.²³ to study the self-assembly of polydisperse spherical nanoparticles of cadmium selenide to clusters with a lower polydispersity of the cluster size. The reduction of polydispersity is a striking result of their work, providing a method for creating uniformly sized building blocks for hierarchical self-assembly.^{1,2} Another type of renormalization for very short-range attractive and long-range repulsive colloids was also proposed by Sciortino et al.¹³, with the difference being that the clusters were treated as monodisperse uniformly dense spherical particles and the renormalization was exponentially dependent on the radius of the spheres. Sciortino et al.¹³ do not simulate the renormalized system but calculate the renormalized repulsion analytically and compare it with the

Received: November 28, 2014

Published: July 23, 2015

purely repulsive Yukawa spheres. In contrast, the model of Xia et al.²³ considers each particle within the cluster explicitly, and the renormalized potentials are regularly updated in their molecular dynamics simulation. In what follows, we define a model, which is based on the advanced model of Xia et al.²³ but is simpler and closer to other well-examined SALR models.^{9,13,14,17} An analogy between these two types of models has already been pointed out by ref 24. Instead of the standard Lennard-Jones attraction of ref 23, we use an attractive range which is about five times shorter, but we preserve the idea of a volume-dependent renormalization of the repulsive term. Shorter-ranged attraction allows us to take advantage of the optimum temperature regions for self-assembly¹⁸ in the phase diagram⁶ and examine the effect of kinetic slowing down resulting from attractive forces. As opposed to the model in ref 23, which uses a system of polydisperse particles, we use monodisperse particles only. We compare the polydispersity of the aggregates generated by potentials with renormalized and non-renormalized repulsive amplitudes.

2. METHODS

2.1. Simulation Model. The underlying potential is based on a generalized Lennard-Jones potential equipped with a Yukawa repulsion

$$V(r) = A \frac{e^{-r/\xi}}{r/\xi} + 4\epsilon \left[\left(\frac{\sigma}{r} \right)^{2\alpha} - \left(\frac{\sigma}{r} \right)^\alpha \right] \quad (1)$$

The parameters of the model were chosen close to those of refs 10 and 14 in order to compare the effects of renormalization with the previous results. The diameter of the particle is $\sigma = 1.0$. The screening length is fixed as $\xi = 2.0\sigma$,^{13,20} and the exponent $\alpha = 18$,^{6,7,25} which corresponds to an attractive well width of approximately 0.2σ . The depth of the well is taken as $\epsilon = 1.0$. A fixed amplitude A in eq 1 is used in preliminary simulations to find parameters for the renormalization of A and to generate reference trajectories for comparison with the renormalization approach (see later). All of the potentials are cut off at a distance equal to $r_c = 3.0\sigma$, and a shift eliminating the discontinuity at r_c is applied.

The rate of change of repulsion with volume is defined as

$$s = \frac{A_f - A_c}{R_c^3 - R_f^3} \quad (2)$$

with quantities A_f , A_c , R_f , and R_c being parameters. The volume of the clusters is calculated in terms of the radius of gyration. The parameter R_c is the average radius of gyration of the desired cluster and is fixed arbitrarily (or according to an experiment); $R_c = \sigma$ is fixed for simplicity and to keep the clusters sufficiently small. The parameter R_f represents the radius of gyration of the non-renormalized unit. In our case it is a single particle. We choose $R_f = 0.48\sigma$. Again, to be close to ref 10, we take the amplitude at which the clusters are long-lived as $A_c = 0.08$. The amplitude A_f at which the clusters rapidly dissolve into a fluid can be estimated in *a priori* simulations. The Results section will show that $A_f = 0.25$. The potential, for values $A = 0$, A_c , and A_f is illustrated in Figure 1.

To define the pairwise potentials with the renormalized A in eq 1, the system needs to be split into clusters. We use a standard definition of a cluster. Two particles are neighbors if they lie at a distance less than 1.4σ . By a cluster we then understand a set of particles C_i , which can be connected via

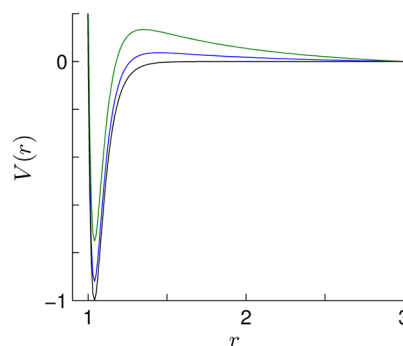


Figure 1. Short-range attractive and long-range repulsive potential in eq 1 with stronger $A_f = 0.25$ (green, top), weaker $A_c = 0.08$ (blue, middle), and zero $A = 0$ (black, bottom) repulsive amplitudes: (in all cases) diameter, $\sigma = 1$; well depth, $\epsilon = 1$; screening length, $\xi = 2.0$; exponent, $\alpha = 18$.

neighbors. The system S can then be divided into n_c clusters, symbolically

$$S = \bigcup_{l=1}^{n_c} C_l = \bigcup_{i=1}^N C_{k_i}, \quad (3)$$

where k_i is the number of the cluster containing particle i , and C_{k_i} is the cluster containing particle i . The idea behind the phenomenological renormalization of the repulsive amplitude is that A in the pairwise potential (eq 1) between particles i and j is chosen depending on the properties of their parent clusters C_{k_i} and C_{k_j} . R_{k_i} and R_{k_j} denote the radii of gyration of C_{k_i} and C_{k_j} . Having obtained A_f and A_c previously, we can calculate the rate of amplitude change in eq 2 and define the renormalized amplitude as

$$A = \begin{cases} A_c & \text{if } k_i = k_j \\ A_c + s \left(\frac{R_{k_i}^3 + R_{k_j}^3}{2} - R_f^3 \right) & \text{if } k_i \neq k_j \end{cases} \quad (4)$$

2.2. Simulation Method. The system is simulated with both conventional single-particle Monte Carlo (SPMC) and virtual move Monte Carlo (VMMC); the latter algorithm moves both single particles and clusters, where clusters are selected according to the local force fields.^{8,26–28} The Monte Carlo simulation makes sure that the attempted move of a particle close to a large cluster is likely to be rejected, because the renormalized repulsive shoulder would result in a large positive potential energy change. The same applies when two large clusters approach each other. If a molecular dynamics simulation was used with our model system, the potential energy would likely become unphysically large after renormalization, and the simulation would blow up.

We use the generalized version of the VMMC algorithm²⁷ to enhance cluster rotations. The maximum displacement is $\delta = 0.2\sigma$. The simulations are performed in the canonical ensemble, with N particles, volume V , and temperature T . The size of the system is $N = 2000$ and packing fraction $\phi = (\pi/6)(N/V) = 0.01$. We find it convenient to measure simulation time as $\tau = n_{\text{sweep}}\delta^2$, where n_{sweep} is the number of MC sweeps. This accounts, in a crude way, for the diffusive nature of single-particle motion in the SPMC case, in the limit of small δ (see the Supporting Information (SI) for further discussion). In

SPMC, a sweep consists of N attempted translational moves. In VMMC, it consists of N virtual translational or rotational moves, with on average $N/2$ translations and $N/2$ rotations. Simulations with the potential in eq 1 and amplitude A defined in eq 4 start from a high-temperature fluid, which is instantaneously quenched to $T = 0.25$, an optimum temperature region for self-assembly.^{7,8,18} Similar parameters have been used elsewhere.¹⁴

The definition of the potentials in eq 4 requires knowledge of the exact position of particles with respect to their clusters at each proposed and accepted Monte Carlo move. This operation is computationally expensive if applied to the whole system but can be accelerated by using dynamical biconnectivity techniques,²⁹ updating the information about clusters according to the local changes.

2.3. Analysis. The time evolution of local crystallinity is analyzed with q_6q_6 “Steinhardt” parameters.^{30,31} If $N_b(i)$ is the number of neighbors of particle i , the local crystallinity can be described by

$$Q_{lm}(i) = \frac{1}{N_b(i)} \sum_{j=1}^{N_b(i)} Y_{lm}(\vec{r}_{ij}) \quad (5a)$$

$$q_{lm}(i) = \frac{Q_{lm}(i)}{(\sum_{m'=-l}^l |Q_{lm'}(i)|^2)^{1/2}} \quad (5b)$$

where $Y_{lm}(\vec{r}_{ij})$ is the spherical harmonic corresponding to the vector \vec{r}_{ij} between particles i and j . We focus on $l = 6$ since this characterizes the predominant structure in these systems.⁷ A neighboring pair (ij) is said to be orientationally bonded if

$$\sum_{m=-6}^6 q_{6m}(i) \bar{q}_{6m}(j) > 0.7 \quad (6)$$

where $\bar{q}_{6m}(j)$ is the complex conjugate of $q_{6m}(j)$. The number of neighbors which are orientationally bonded to i is denoted as $N_b(i)$. A particle is crystalline if $N_b(i) > 10$. A group of at least two bonded crystalline particles will be called a *crystal*. A group of at least two particles with $N_b(i) > 5$ will be called a low symmetry cluster (LSC). In analogy to Schilling et al.,³¹ we distinguish between LSCs with and without a crystal inside. An LSC with a crystal is different from a crystal, in that it also includes any particles in the partially ordered surface of the crystal. Such an LSC may actually contain multiple crystals which are connected together by partially ordered layers of particles. We monitor the time evolution of the local crystallinity and the cluster size distribution. Since only 10 independent simulations are done for each system in this study, the statistics about the cluster size distribution are rough, especially for the non-normalized system, where the phase separation results in two or three large clusters. We thus found it appropriate to plot the size of the six largest clusters. These plots also enable us to relate the growth rates to the structural properties of the system which vary during the course of the phase separation.¹⁰

3. RESULTS

3.1. Determination of Model Parameters. The *a priori* simulations determining A_f and A_c are performed with SPMC simulations with $\delta = 0.1\sigma$ for simplicity. The simulations start from a configuration composed of several separate clusters. The quantity A_c is then defined as the largest A such that the system

does not dissolve. We took $A_c = 0.08$ to be close to that of ref 10, although a slightly higher value is possible. The quantity A_f is defined as the smallest A such that the system rapidly dissolves into a fluid. We took $A_f = 0.25$. Figure 2 shows that a

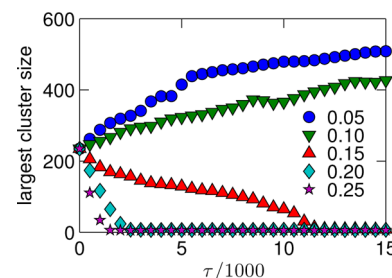


Figure 2. Size of the largest cluster of the system in SPMC simulations for different values of the repulsion A .

slightly lower value of A_f can also be chosen. Lower values of A_f however, lead to larger clusters in the system with renormalized repulsion amplitude studied in the next section.

The properties of the system under different choices of A can be characterized as follows. If $A_f < A$, the system dissolves rapidly into a stable fluid state. If $A_c < A < A_f$, the system is in a metastable state characterized by a short-time-scale existence of the metastable aggregates. If $A < A_c$, then, depending on the size of A , the system is either in the stable cluster phase or in the crystal phase. We note that the thermodynamic stability of cluster phases can be hard to verify and that the cluster phase we observe may actually be a metastable state persisting on a time scale much longer than the states for $A_c < A < A_f$. We emphasize that this work aims to examine properties of a crude renormalization model and that exact values of parameters A_f and A_c , determining the parameter s , are not essential.

3.2. Kinetically Slowed down Phase Separation. Figure 3 compares the structure evolution in the SALR system without and with the volume-dependent renormalization in a kinetically slowed down phase separation.

As has been shown previously in ref 10, the phase separation can be characterized by growth regimes, where the local structure is correlated with the speed at which the cluster grows. Figure 3a captures a regime which exhibits rapid growth of disordered clusters. This regime is terminated when the concentration of weakly bonded particles ($N_b(i) = 2$) reaches a maximum. The local crystallinity then starts evolving rapidly in another regime where disordered clusters dissolve at the expense of growing clusters which have a higher degree of crystallinity. The primary mechanism of this rapid emergence of crystalline particles is particle detachment from an amorphous cluster and its attachment to a crystalline surface of an ordered cluster. Figure 3c then shows that LSCs contain more than one crystal, meaning that amorphous surfaces of LSCs with a crystal inside act as nucleation sites for new crystals.

The renormalization of the long-range repulsion leads to the stabilization of smaller aggregates, with the resulting clusters having roughly the same size compared to the highly polydisperse aggregates in the non-renormalized SALR potentials. Nevertheless, the crystallization picture changes dramatically, in that the clusters grow but do not dissolve easily. This is because a particle may surmount the renormalized barrier, and stick to the cluster, but to leave a cluster is energetically unfavorable due to the large potential difference between the bottom of the attractive well and the renormalized

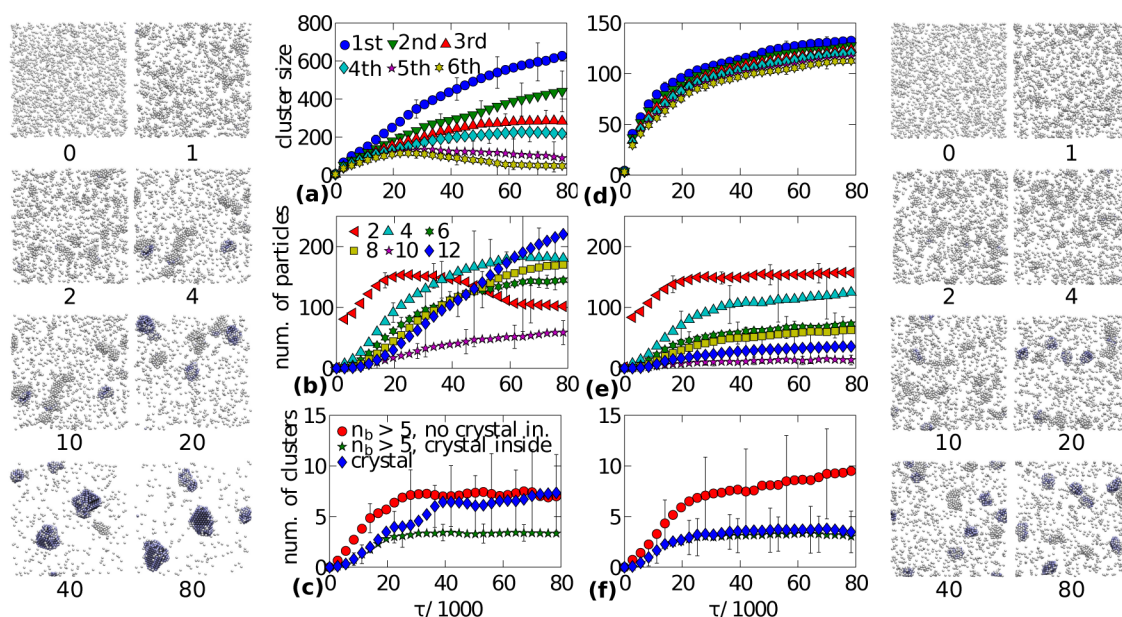


Figure 3. Time evolution of the SALR system composed of particles with short-range attraction and long-range repulsion (eq 1). Time is measured in terms of $\tau = n_{\text{sweep}} \delta^2$ as discussed in the text. The long-range repulsion is not normalized ($A = A_c$) in the sequence on the left and is normalized (given by eq 4) in the sequence on the right. The simulation is started from a quenched liquid state. Particles are colored according to the local crystal order: white (isolated or amorphous with low $N_b(i)$), blue (surface particles with intermediate $N_b(i)$), dark gray (crystalline with high $N_b(i)$). The graphs show the evolution of long- and short-range structures. (a and d) Size of the six largest clusters in the system. (b and e) Local order measured by the number of particles with a fixed number of orientational bonds given in the legend. (c and f) Number of crystals (diamonds), low symmetry clusters with no crystals inside (circles), and low symmetry clusters with crystals inside (stars). All error bars are averages from 10 independent simulations.

repulsive shoulder. The dynamics of phase separation is shown again in Figure 3. The initial regime, characterized by a rapid clustering into ordered and unordered clusters, remains quantitatively nearly identical to the system with non-renormalized repulsion. The two models start to deviate only at the end of this regime, when amorphous clusters do not dissolve, and crystal surfaces of other clusters do not grow. This is indicated by the roughly constant number of particles with few orientational neighbors, and the very slow growth of higher-ordered local structure, reflecting a structural arrest in the form of a repulsive or attractive glass transition within the clusters. Figure 3f shows that an LSC with a crystal inside usually contains just one such crystal and that the number of those clusters remains constant at later times. This confirms that the crystallinity does not evolve in the later stages, but it also suggests that the clusters do not merge, and remain isolated, thus preserving the monodispersity. Parts d and f of Figure 3 then show that clusters slowly coarsen, that no new crystals form, and that local order within the unordered regions evolves slowly. The result is then a long-lived state of monodisperse clusters, some of which are crystalline and others amorphous. Results for a larger system are similar (see the SI).

The time evolution of cluster size distribution is plotted in Figure 4 and confirms a relatively narrow cluster size distribution in the renormalized system. The distribution develops a peak for larger clusters at late times showing that smaller-sized clusters grow to larger clusters. The drop in the number of smaller-sized clusters is not present in the non-normalized system since the larger clusters not only grow but can also dissolve more easily, as discussed earlier. Both normalized and non-normalized systems are characterized by the coexistence of several large clusters and significantly higher

number of single particles or small-sized clusters even at late times of the simulation, suggesting that the equilibrium phase of the system is a solid phase coexisting with gas.

The size distribution of clusters with different structural properties is quantitatively similar to the one observed in the suspensions of hard-sphere systems.³¹ The prevailing large clusters are the LSC with crystals inside. The width of their size distribution is nearly invariant with time, with the average cluster size moving to higher values indicating a nearly uniform growth. The size of the largest LSCs with no crystal is comparable to the average size of the LSC with crystal, at the two different times, also indicating the uniform growth. The concentration of large LSCs without crystals grows in the renormalized system, as opposed to the non-normalized system.

4. DISCUSSION

It has been shown that a simple renormalization of the repulsive amplitude reduces the polydispersity of clusters in a system that is different from that studied in ref 23. This is simply because particles are unlikely to approach and reach the attractive surface of larger clusters which have stronger repulsions than small clusters. The renormalization may represent various physical phenomena^{32–34} behind the long-range repulsive forces of larger clusters and may generally reduce the polydispersity of clusters in phase-separating systems. The linear dependence of the amplitude on the volume of the cluster is an attempt to make a first-order approximation of the renormalization.

Since pairwise interactions *within* a cluster are not renormalized in either model of Figure 3, and since the number of particles with high N_b grows significantly faster in the model without the renormalization, it can be concluded that

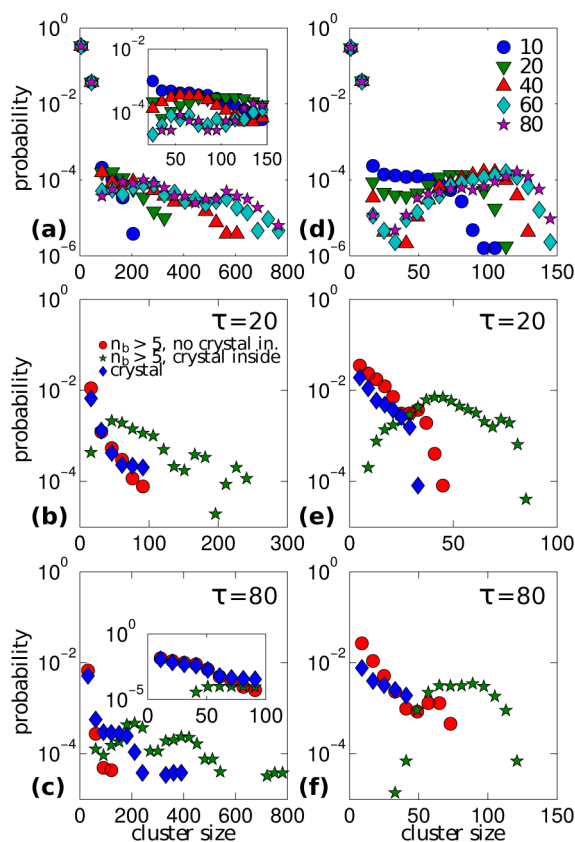


Figure 4. Time evolution of cluster size distribution for non-normalized repulsion (left) and the renormalized system (right): (a and d) size distribution of all clusters at times specified by the legend of d; (b, c, e, and f) time evolution of clusters with structure specified by the legend of b at fixed times $\tau = 20$ and $\tau = 80$. The insets of a and c show the distribution of small clusters in the respective plots.

the evolution of local order within disordered regions inside the cluster is very slow compared to the evolution of local order via the growth of crystalline surfaces. Indeed, it was shown before that small clusters are less stable in the non-renormalized system and that the growth of the crystalline surfaces on the larger clusters happens at the expense of particles from the dissolved clusters. It is now interesting to discuss the relaxation process inside the amorphous clusters, because the long-range repulsion may destabilize the central part of the dense regions. We illustrate this by considering an ideally spherical and sufficiently large cluster, composed of short-range attractive particles with a repulsion, the range of which is equal to at least the diameter of the cluster. The contribution of the total long-range potential of the particles near the surface to the particle in the center of the cluster is large, and such a particle is in an energy maximum; i.e., the energy per particle in the center of the cluster is higher than the energy per particle on the surface.¹⁰ It is thus reasonable to expect that the body density²² of the cluster may not be constant and may be locally lower in the core than in the surface. This may have two consequences. The lower body density may ease the relaxation of a glassy region around the center of the cluster and move it closer to the optimum region for self-assembly.¹⁸ The center may thus crystallize. However, if the contribution from the long-range forces is large enough, the central part of the cluster may dissolve, and become fluid-like. This scenario is plausible in a model system with a screening length which is independent of

the fluctuations in the colloidal density. The SI provides some numerical evidence that the long-range repulsion in our non-normalized system leads to the relaxation of the arrested region inside the cluster.

The original renormalization of the potentials by Xia et al.²³ is more complex and distinguishes between the screening length, ξ , inside and outside the cluster, mostly in order to facilitate relaxation of the particles inside the cluster. The model also considers different screening lengths for differently sized clusters with the critical size being given by R_c , and different pairwise interactions inside and outside the disordered surfaces of the forming clusters. For simplicity, and in analogy to most other studies,^{12–14,20,21} these distinctions were not made here; nonetheless, the internal structure of the clusters may relax easily. It is also shown that the model of ref 23 may have missed the important crystallization mechanism, based on the dissolution of amorphous drops and consequent growth of amorphous surfaces. A more detailed analysis would be needed to show whether consideration of different interactions in the core and in the shell of the cluster eases the dissolution process.

The work of Sweatman et al.²² may suggest that the model of Xia et al.²³ use a longer-range repulsion and that amorphous drops recrystallize quicker than they dissolve. Nevertheless, the work of Sastry³⁵ shows that kinetic arrest happens even if the attraction is longer-ranged. The dissolution of amorphous regions and their subsequent recrystallization may thus be a viable mechanism for relaxation. Whether consideration of different screening lengths inside and outside the cluster is a necessary and correct approximation to model relaxation within amorphous regions, and what is the effect of long-range contribution from the surface to the center of the cluster, all require further investigation.

These renormalized long-range forces may not only represent screened electrostatic repulsion^{13,34} but also steric repulsion,³² where polymeric chains decorate the particle, or generally accumulation repulsion,³³ where polymers or other particles of the system interact with the self-assembling colloids. The model of Xia et al.,²³ and the model of this work may still be improved by renormalizing the amplitude according to Denton,³⁴ and with respect to the center of mass of the cluster.¹³ The renormalized potentials defined in eq 4 do not work at high packing fractions close to gelation, because the center of mass and the radius of gyration become undefined whenever the clusters or particles percolate. However, the current potential form should still allow one to compress or simulate the system at lower packing fractions when attractive percolation is unlikely to occur and to investigate the properties of the resulting cluster phase, which, if arrested, is known as the Wigner glass.¹³ The cluster size is known to increase with packing fraction in the non-renormalized model^{5,13} and remain constant in the renormalized model.²³ We note that we may expect the clusters to be smaller if the repulsion rate with volume is increased. Also, for quenches to lower temperatures, the size would be determined by the competition of the attractive term ϵ and the renormalized repulsion A .

The renormalization-based models may express the intra- and intercluster interactions in a more realistic way than standard SALR models, which assume that the screening length is the same inside the cluster and in the solvent. Disadvantages of the renormalization are the large computational expense of repartitioning the system into clusters at every Monte Carlo step and the fact that the parameter R_c and an assumption of roughly spherical clusters are required. The non-renormalized

SALR models^{13,14} are thus still a viable option to investigate the polydispersity of clusters in SALR systems. Advanced simulation or preparation protocols, such as controlled quenches,³⁶ adjustments of temperatures,³⁷ or displacements δ ,¹⁰ may be alternative approaches to investigate cluster polydispersity. Indeed, by a systematic dispersion of clusters in a system of particles interacting via non-renormalized SALR potentials, Sweatman et al.²² show that the thermodynamic state is characterized by large spherical clusters with low polydispersity of cluster size.

The volume-dependent repulsion model may be suitable to simulate the kinetics of low-density cluster (Wigner) crystals,¹³ but its current form is a crude and computationally expensive approximation requiring *a priori* simulations and a parameter defining the size of the desired cluster. Moreover, the necessity to partition the system to define the potentials makes it impossible to model gelation¹¹ or arrest at high densities.^{1,2} A definition of a computationally tractable and accurate physical model describing the formation of monodisperse clusters and their hierarchical self-assembly into high-density structures thus remains an open problem.

5. CONCLUSIONS

We have generated and analyzed an ensemble of pathways of phase separation in a low-density SALR system following a shallow quench^{6,7} to the temperature region below the critical point, where conditions for good assembly are expected.¹⁸ The system phase separates into several isolated drops, some of which are crystalline and others amorphous.¹⁰ The long-range repulsion inhibits the aggregation of those drops into a single aggregate, and the drops may live for a very long time. We compare behavior of the system under two forms of pairwise long-range repulsion, which underlies the large repulsive shoulder of a cluster. The first form is a simple pairwise repulsion^{12–15,17,21,22} with the corresponding cluster repulsion being merely formed by a sum of repulsive contributions of particles in the cluster. The second form of the repulsion also adds up the pairwise contributions from particles in the cluster, but the magnitude of the pairwise contributions is linearly proportional to the volume of the cluster.²³ This makes the latter form of cluster repulsion stronger than the former, with the volume dependence significantly promoting the monodispersity of the clusters.

The model of cadmium selenide nanoparticles²³ assumed a more complicated form of the linear dependence to explain the monodispersity of the aggregates. Here, we show that even a simple form of volume-dependent long-range repulsion is sufficient to decrease the polydispersity. We put the model into the context of nonclassical crystallization, and we discuss the role of kinetic slowing down,⁷ and the role of amorphous and crystalline clusters.¹⁰ We show that the volume-dependent renormalization significantly slows down the crystal formation due to the high stability of amorphous clusters, which would have been dissolved in the classical non-renormalized SALR model.

Polydispersity of aggregates is decreased in a model which is simpler but fundamentally similar to the model of ref 23, in that the repulsion is linearly proportional to the volume of the cluster. The linear dependence is a crude approximation with a phenomenological basis. We conclude that a computationally tractable model, with sound physical foundations explaining the monodispersity of CdSe clusters, remains an open question.

■ ASSOCIATED CONTENT

§ Supporting Information

The Supporting Information is available free of charge on the ACS Publications website at DOI: 10.1021/ct501067t.

Additional details of some technical issues, which are related to the Monte Carlo simulations and to the finite size effects (PDF)

■ AUTHOR INFORMATION

Corresponding Author

*E-mail: stepan.ruzicka@u-psud.fr.

Funding

This work was supported by the Engineering and Physical Sciences Research Council (Grant No. EP/I001514/1). This Programme Grant funds the Materials Interface with Biology (MIB) consortium.

Notes

The authors declare no competing financial interest.

■ ACKNOWLEDGMENTS

We thank Trung Nguyen for correspondence describing the renormalization in the model of ref 23 and David Quigley, Martin Sweatman, Alessandro Troisi, and Bart Vorselaars for discussions. We thank the Centre for Scientific Computing of the University of Warwick for computational resources.

■ REFERENCES

- (1) Leite, E. R.; Ribeiro, C. *Crystallization and Growth of Colloidal Nanocrystals*; Springer: New York, NY, USA, 2012.
- (2) Cölfen, H.; Antonietti, M. *Mesocrystals and Nonclassical Crystallization*; Wiley: Chichester, U.K., 2008.
- (3) Zhou, L.; O'Brien, P. J. *Phys. Chem. Lett.* **2012**, 3, 620.
- (4) ten Wolde, P. R.; Frenkel, D. *Science* **1997**, 277, 1975.
- (5) Stradner, A.; Sedgwick, H.; Cardinaux, F.; Poon, W. C. K.; Egelsafer, S. U.; Schurtenberger, P. *Nature* **2004**, 432, 492.
- (6) Vliegthart, G. A.; Lodge, J. F. M.; Lekkerkerker, H. N. W. *Phys. A* **1999**, 263, 378.
- (7) Perez, T.; Liu, Y.; Li, W.; Gunton, J. D.; Chakrabarti, A. *Langmuir* **2011**, 27, 11401.
- (8) Whitelam, S.; Feng, E. H.; Hagan, M. F.; Geissler, P. L. *Soft Matter* **2009**, 5, 1251.
- (9) Charbonneau, P.; Reichman, D. R. *Phys. Rev. E* **2007**, 75, 011507.
- (10) Růžička, Š.; Allen, M. P. *Eur. Phys. J. E: Soft Matter Biol. Phys.* **2015**, 38, 154.
- (11) Lu, P. J.; Zaccarelli, E.; Ciulla, F.; Schofield, A. B.; Sciortino, F.; Weitz, D. A. *Nature* **2008**, 453, 499.
- (12) Charbonneau, P.; Reichman, D. R. *Phys. Rev. E* **2007**, 75, 050401(R).
- (13) Sciortino, F.; Mossa, S.; Zaccarelli, E.; Tartaglia, P. *Phys. Rev. Lett.* **2004**, 93, 055701.
- (14) de Candia, A.; Del Gado, E.; Fierro, A.; Sator, N.; Tarzia, M.; Coniglio, A. *Phys. Rev. E* **2006**, 74, 010403(R).
- (15) Archer, A. J.; Wilding, N. B. *Phys. Rev. E* **2007**, 76, 031501.
- (16) Zhang, T. H.; Klok, J.; Tromp, R. H.; Groenewold, J.; Kegel, W. K. *Soft Matter* **2012**, 8, 667.
- (17) Mani, E.; Lechner, W.; Kegel, W. K.; Bolhuis, P. G. *Soft Matter* **2014**, 10, 4479.
- (18) Klotz, D.; Jack, R. L. *Soft Matter* **2011**, 7, 6294.
- (19) Mossa, S.; Sciortino, F.; Tartaglia, P.; Zaccarelli, E. *Langmuir* **2004**, 20, 10756.
- (20) Toledano, J. C. F.; Sciortino, F.; Zaccarelli, E. *Soft Matter* **2009**, 5, 2390.
- (21) Malins, A.; Williams, S. R.; Eggers, J.; Tanaka, H.; Royall, C. P. *J. Non-Cryst. Solids* **2011**, 357, 760.

- (22) Sweatman, M. B.; Fartaria, R.; Lue, L. *J. Chem. Phys.* **2014**, *140*, 124508.
- (23) Xia, Y.; Nguyen, T. D.; Yang, M.; Lee, B.; Santos, A.; Podsiadlo, P.; Tang, Z.; Glotzer, S. C.; Kotov, N. A. *Nat. Nanotechnol.* **2011**, *6*, 580.
- (24) Clancy, P. *Nat. Nanotechnol.* **2011**, *6*, 540.
- (25) Sciortino, F.; Tartaglia, P.; Zaccarelli, E. *J. Phys. Chem. B* **2005**, *109*, 21942.
- (26) Růžička, Š.; Allen, M. P. *Phys. Rev. E* **2014**, *89*, 033307.
- (27) Růžička, Š.; Allen, M. P. *Phys. Rev. E* **2014**, *90*, 033302.
- (28) Whitelam, S. *Mol. Simul.* **2011**, *37*, 606.
- (29) Henzinger, M. R. *Algorithmica* **1995**, *13*, 503.
- (30) Steinhardt, P. J.; Nelson, D. R.; Ronchetti, M. *Phys. Rev. B: Condens. Matter Mater. Phys.* **1983**, *28*, 784.
- (31) Schilling, T.; Schöpe, H. J.; Oettel, M.; Opletal, G.; Snook, I. *Phys. Rev. Lett.* **2010**, *105*, 025701.
- (32) Likos, C. N.; Löwen, H.; Watzlawek, M.; Abbas, B.; Jucknischke, O.; Allgaier, J.; Richter, D. *Phys. Rev. Lett.* **1998**, *80*, 4450.
- (33) Louis, A. A.; Allahyarov, E.; Löwen, H.; Roth, R. *Phys. Rev. E: Stat. Phys., Plasmas, Fluids, Relat. Interdiscip. Top.* **2002**, *65*, 061407.
- (34) Denton, A. R. *J. Phys.: Condens. Matter* **2008**, *20*, 494230.
- (35) Sastry, S. *Phys. Rev. Lett.* **2000**, *85*, 590.
- (36) Royall, C. P.; Malins, A. *Faraday Discuss.* **2012**, *158*, 301.
- (37) Klotsa, D.; Jack, R. L. *J. Chem. Phys.* **2013**, *138*, 094502.